

An intelligent strabismus detection method based on convolution neural network

Haider Shamil Hamid¹, Bassam AlKindy¹, Amel H. Abbas¹, Wissam Basim Al-Kendi²

¹Department of Computer Science, College of Science, Mustansiriyah University, 10001 Baghdad, Iraq

²Federal Commission of Integrity, 10001 Baghdad, Iraq

Article Info

Article history:

Received Apr 28, 2021

Revised Jun 04, 2022

Accepted Jun 26, 2022

Keywords:

Convolutional neural networks

IMPA-FACE

Strabismus

Vision disorders

ABSTRACT

Strabismus is one of the widespread vision disorders in which the eyes are misaligned and asymmetric. Convolutional neural networks (CNNs) are properly designed for analyzing images and detecting texture patterns. In this paper, we proposed a system that uses deep learning CNN applications for automatically detecting and classifying strabismus disorder. The proposed system includes two main stages: first, the detection of facial eye segmentation using the viola-jones algorithm. The second stage is to map the segmented eye area according to the iris position of each eye. This method is applied to three strabismus datasets, gathered as digital images. The second section covers the segmentation of the eye region. Besides, the evaluation equations for measuring system performance. The system has undergone numerous experiments in various stages to simulate and analyze the detection performance of CNN layers through different classifiers and variant thresholds ratio. The researchers investigated the experimental outcomes during the training and testing phases and obtained promising results that exhibit the effectiveness of the proposed system. According to the results, the accuracy of this technique reached 95.62%.

This is an open access article under the [CC BY-SA](https://creativecommons.org/licenses/by-sa/4.0/) license.



Corresponding Author:

Bassam AlKindy

Department of Computer Science, College of Science, Mustansiriyah University

Palestine Street, 10001 Baghdad, Iraq

Email: dr.balkindy@uomustansiriya.edu.iq

1. INTRODUCTION

Strabismus is an eye disease in which the iris of the eye cannot align in the same position [1], which occurs often in childhood. Mainly, It is caused by a problem occurring in the optic-nerve, brain, or extraocular muscle [2]. Dangerous factors include familial inheritance [3] and early births underlying strabismus disease which has a severe impact on human life. In addition, it can prevent the brain from fusing the images collected by the two eyes, which leads to amblyopia [4]. Untreated seeing eyes can degenerate, leading to blindness [5]. In addition, double vision and deep insight of strabismus patients is lower than that of healthy people. Therefore, the prognosis and treatment of strabismus becomes increasingly important where the detection of strabismus is the first and one of the essential steps. The traditional approaches to detecting strabismus are usually done in hospitals. Doctors of patients with strabismus use the hirschberg test [6] to determine if the patient has strabismus: a thin beam of light is sent into the patient's eye to check if each ocular reflex is in the same place on both corneas. As the number of patients with strabismus increases, the detection of strabismus mainly becomes annoying and prostrate with error. However, automatic detection is a useful and practical approach to alleviate the growing demand for detection of strabismus [7], Horner *et al.* [8] uses telemedicine to diagnose strabismus in places where specialists are not available. In such a situation, patient images were taken by high-resolution digital cameras and then sent to specialists for remote analysis and determination of strabismus.

In addition, some methods of detecting strabismus with digital tools are used. Attada *et al.* [9] uses photorefracton to achieve narrow angle strabismus detection. Loudon *et al.* [10] use the pediatric vision scanner to detect strabismus. Almeida *et al.* [11] applies a digital camera and the Hirschberg test to identify strabismus. Valente *et al.* [12] carry out the detection of strabismus in digital videos using coverage tests. Chen *et al.* [13] use an eye tracking system and convolutional neural networks to detect strabismus. Most of the previous studies use eye and eye tracking devices to capture the position of the iris or high-resolution images captured by digital cameras. In addition, the classification step did not lead to classifying the type of strabismus. In this article, deep neural network models are used to perform automatic detection of strabismus and specify the type of strabismus according to different sources of image acquisition (for example, low to high resolution of digital images). In recent years, deep neural networks have increased, as an efficient deep neural network training algorithm [14]–[20]. The rest of this paper as: section 2 will highlight the theoretical part of the proposed method. Section 3 gives the main results obtained from considering three datasets. Section 4 provides a conclusion of this study.

2. METHOD

2.1. Dataset

Three datasets are used in this work in a total of 285 human facial images. The first dataset as shown in Figure 1(a) is captured by utilizing a low-resolution camera (i.e. laptop or mobiles camera) with a metal stand for aligning the face angle within the camera. The second dataset, as Figure 1(b), obtained from ophthalmologists, where all images collected from patients using mobile phones, and the third dataset obtained from previous studies called impa-faced dataset [21] as illustrated in Figure 1(c). All datasets images are scaled to a fix coordination (e.g. 640×480 pixels). To acheive the automated strabismus detection, datasets are carefully annotated by ophthalmologists. For model learning purposes, we divided the datasets into two subsets: a training set contains 205 patients images (represents 72%) and a testing set contains 80 patients images (represents 28%).

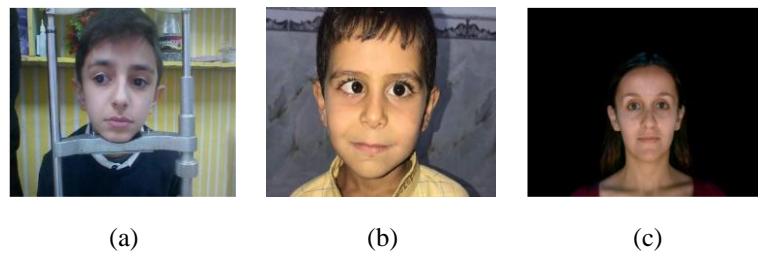


Figure 1. Sample images from datasets: (a) strabismus image from the real captured dataset, (b) strabismus image from the dataset collected by specialists, and (c) the normal vision from impa-faced dataset

2.2. Proposed model

In this work, the proposed model uses the convolutional neural network (CNN) to acquire deeply the features vector for automatic strabismus detection. The model is consisting of two stages: firstly, the eye region segmentation from the face is performed using the viola-jones algorithm [22]. Secondly, map the segmented eye regions into two output classes (strabismus: 1 or normal: 0) according to each eye iris position. The general flow diagram of the detection method illustrated in Figure 2.

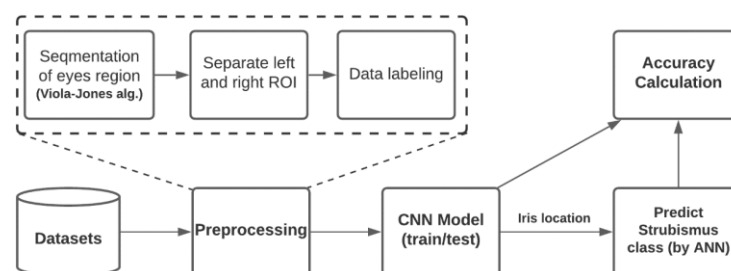


Figure 2. The general framework of the proposed algorithm

2.3. Segmentation of eye region

Applying three datasets from different sources will enhance the model training stage. Strabismus detection depends primarily on the discovery of eye regions from the human face. For this purpose, we applying the viola-jones algorithm to detect the eye region from the patient face [23]. Further, we select a pre-trained classifier model from a pool of classifiers to identifying eye pair location while the face is aligned in front of the camera using a metal stand. The algorithm detects the region of eye pair in rectangular form based on the coordination points (x, y, w, h) , where (x, y) represent the point of rectangular eye region top-left position, and (h, w) stands for the rectangular height and width respectively. Note, the values of the rectangular eye region shape are in pixels. Deeply speaking, a detector detects the eye region object using a sliding window over the input image. The size of the window could be adjusted for detecting objects at various scales; however, the aspect ratio remains the same. The stages of the classifier are designed to remove the negative pieces from an image. At this point, we get a bounding box from applying haar features (shortly HF) to detect the eyes pair region. Consequently, it results in extracting the eye pair with the class number. Figure 3 illustrates instances of segmented eye pair regions.

2.4. Separation of eye region

After obtaining the eye region as Figure 3, the next step is to separate left and right eye segments. For strabismus detection, both separated models would be of the same size. Practically speaking, after separation we resized each image to 42×22 pixels and fed it to CNNs as a training set. The target class number will map the position of the eye iris (e.g. 0: center, 1: left, and 2: right) as Figure 4(a) and Figure 4(b).

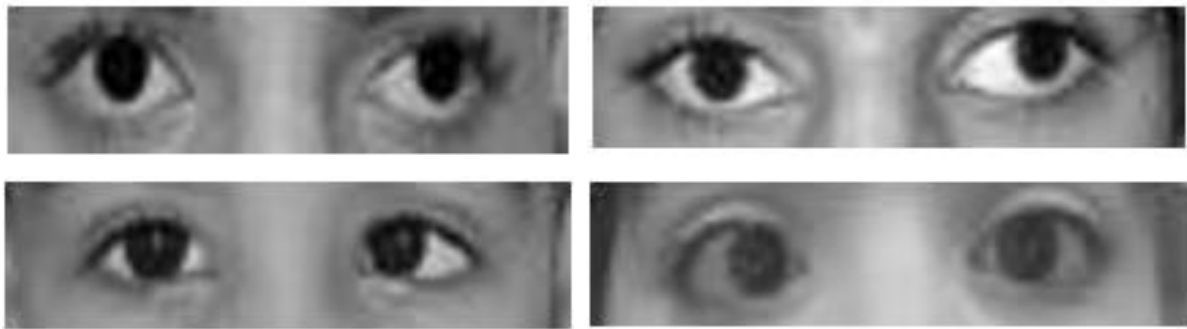


Figure 3. Exemplary instances of segmented eye pair regions

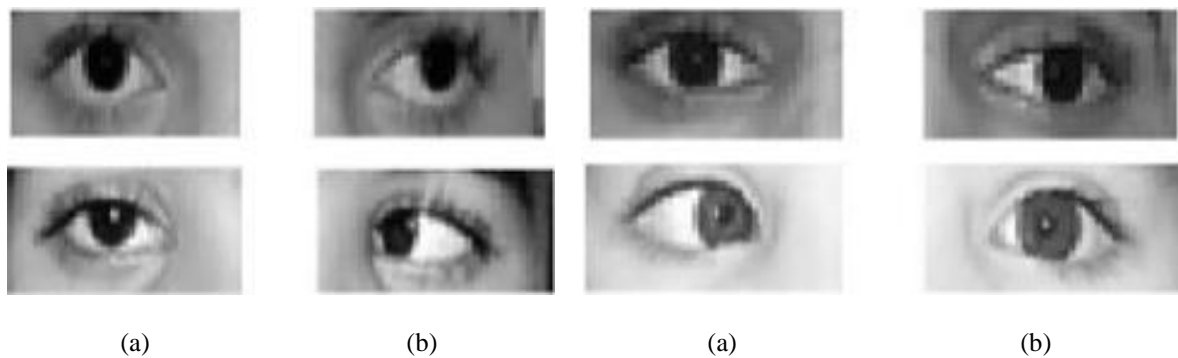


Figure 4. Segmented instances of (a) right and (b) left eye pair regions

2.5. Establishing convolution neural network

After separating the eye regions, a deep learning CNN is formed to classify the eye regions. CNN is made up of several neurons arranged or arranged in rectangular layers [24]. The spatial arrangement of neurons is the fundamental property of CNNs, which allows CNNs to be used in a variety of applications. Moreover, sparse connectivity, sharing of settings, and pooling are the other essential properties of CNN.

2.5.1. Sparse connectivity

Sparse connectivity shows that every neuron within the CNN is attached to a small location of neurons within the preceding layers or the following layer. It is performed with the aid of using the use of a kernel decrease than the enter. For example, whilst acting photograph classification, the enter photograph may also have a number of pixels. However, only some beneficial features, inclusive of aspect and shape, are detected with the aid of using kernels. Sparse connectivity can lessen the quantity of saved parameters, that's of incredible significance to the performance of the network.

2.5.2. Parameter sharing

To improve the proposed model detection and execution time, all the neurons that sharing the same layer will share the same layer's parameters. In other words, calculating one set of parameters is sufficient instead of computing separate parameters set for a new location. Hence, the model will have the ability to highlight patterns that are tilted, slightly warped, or shifted within input images.

2.5.3. Pooling

Pooling Indicates that rather than doing convolution, the gatherings of the neuron's output are performed. Max-pooling is the recommended usage of the pooling function that aggregates the neurons and returns the highest value from a rectangular region. Generally speaking, the structure of CNN is usually composed of numerous convolutional and pooling layers, ended with one or many linked layers. Convolutional layers are applied to discover vital features, while the pooling layers are used to keep task-associated data and ignore inappropriate items [25]. Fully linked layers are mapping the excitations to the output neurons, each excitation is mapped to one target class.

2.6. Network architecture and training parameters

In this paper, two models of CNNs have been developed. The first model preserved for classifying the left eye images, and the second model is used for the right eye images. The architecture of both CNN models is composed of two convolutional layers and followed by two pooling layers. Each convolutional layer is followed by one pooling layer that using the rectified linear activation unit (ReLU) activation function [26]. ReLu is an activation function beneficial to optimize the quality of the network. Figure 5 shows three fully connected CNN layers. To avoid over-fitting, the dropout strategy [27] applied in network layers. It is worth mentioning that each convolutional layer has a batch normalization layer. It acts as a regularizer to accelerate network training 14 times [28]. We apply the stochastic gradient descent method [29] for training the network. In addition, regularization with weight decay is used for network training. The ratio of the dropout sets to 0:5 and the learning rate sets to 0.002.

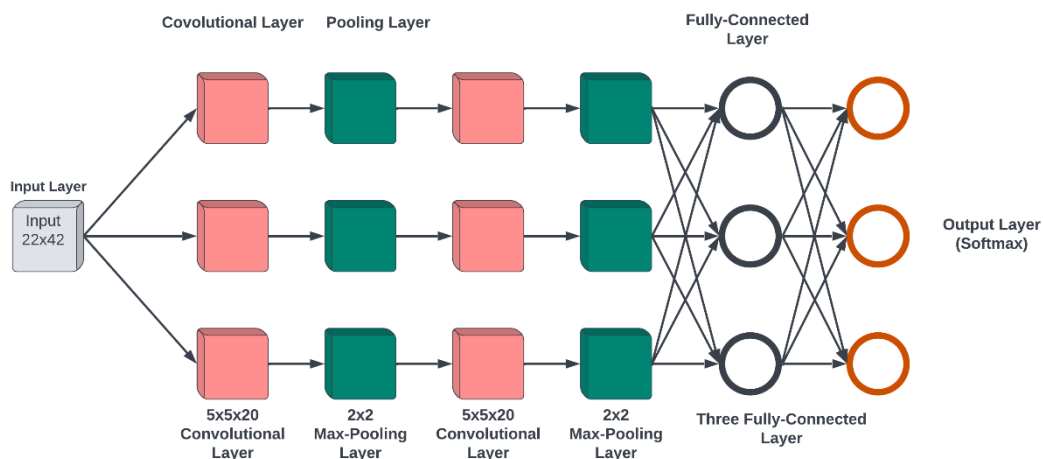


Figure 5. Architecture of CNN network

2.7. Evaluation metrics

To evaluate the performance of the model, we intend to apply three well-known evaluation metrics. These metrics are sensitivity (Se), specificity (Sp), and accuracy (Acc) as shown in:

$$Sensitivity(Se) = \frac{TP}{TP+FN} \quad (1)$$

$$\text{Specificity}(Sp) = \frac{TN}{TN+FP} \quad (2)$$

$$\text{Accuracy}(Acc) = \frac{TP+TN}{TP+TN+FP+FN} \quad (3)$$

In these metrics, true positive (TP) representing the numbers of correctly identified strabismus images, true negative (TN) represents the correctly identified normal images. False positive (FP) that means the incorrectly identified strabismus images. The false negative (FN) is for bad identification of normal images. Se and Sp are responsible to give an algorithm the ability to classify normal and strabismus images from one hand. Acc reflects the classification performance [30] in the other hand.

3. RESULTS AND DISCUSSION

In this section, we conducted two experiments, after the training of CNN models, to evaluate the quality of network outcomes. The first experiment is to monitor the performance of CNN detection layers of iris position based on two classification classes. The second experiment simulates the detection efficiency of various classifiers when providing CNN accuracy and mean square error. It illustrates the accuracy of the matching results from three image classes using the CNN and the classes of images already labeled. Finally, we conducted a focused comparison with other studies.

3.1. Training of CNN models

For training the CNN models based on the training datasets for left and right eye regions, we apply statistical measurements: the accuracy and the mean square error (MSE). For the left eye, the accuracy of training achieves 100%, and the MSE is 0.0201. Table 1 shows these outcomes. For the right eye, accuracy achieves 100%, and mean square error equals 0:0328 as illustrated in Table 2.

Table 1. The training stage of CNN model for left eye images

Epoch	Iteration	Time elapsed (hh: mm: ss)	Mini-batch accuracy (%)	Mini-batch loss	Base learning rate
1	1	00:00:00	20.31	1.5670	0.0020
50	50	00:00:17	98.44	0.0657	0.0020
100	100	00:00:36	99.22	0.0316	0.0020
150	150	00:00:57	100.00	0.0201	0.0020

Table 2. The training stage of CNN model for right eye images

Epoch	Iteration	Time elapsed (hh: mm: ss)	Mini-batch accuracy (%)	Mini-batch loss	Base learning rate
1	1	00:00:00	39.84	1.2926	0.0020
50	50	00:00:20	96.88	0.1237	0.0020
100	100	00:00:39	99.22	0.0596	0.0020
150	150	00:00:59	100.00	0.0328	0.0020

Figure 6 shows the state of accuracy with respect to the number of iterations for left and right eyes in the training stage. In the first epoch, the accuracy was 20.31%. In epoch 50, the accuracy raised to 96.88%. In epoch 100, the accuracy reached 99.22%, and in the final epoch, the accuracy achieves 100%. For the right eye, the final accuracy achieves 100%, and the mean square error equals 0:0328.

Figure 7 shows the state of mean squared error in training state with respect to the number of iterations. For left eye, epoch one started by a mean square error of 1.5670, in epoch 50, the mean squared error decreased to 0.0657, in epoch 100, the mean square error was 0.0316, and in the final epoch, the mean squared error value recorded 0.0201. For right eye, shows the state of mean square error in training state, wherein epoch one, the mean square error was 1:2926, in epoch 50, the mean squared error reaches to 0:1237, in epoch 100 the mean square error is 0:0596, and the last epoch, the mean square error achieves 0:0328. We observed that as the training samples increase, the accuracy of both CNNs increases. In less than 100 training patterns, the detection results improve significantly with the rise of training patterns. Applying over 100 training samples for training the model, we noticed that the detection results are varying insignificantly with the increasing amount of training patterns. From the above observations, 205 training patterns are selected for training CNN. The CNN architecture is illustrated in Table 3.

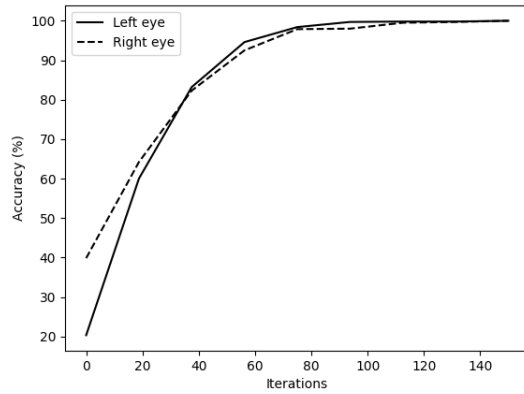


Figure 6. The accuracy of training state of CNN model of left and right eyes

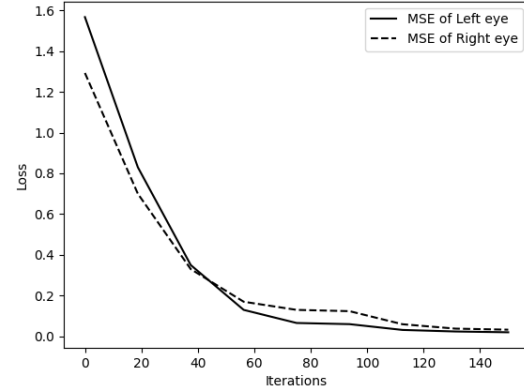


Figure 7. Mean square error of training stage of CNN model for left and right eyes

Table 3. The architecture of the CNN model

Layer no.	Layer name	Type	Activations	Learnables
1	Imageinput 22×42×1 images with 'zerocenter' normalization	Image input	22×42×1	-
2	Conv_1 20 5×5×1 convolutions with stride [1 1] and padding [0 0 0 0]	Convolution	18×38×20	Weights 5×5×1×20 Bias 1×1×20
3	Batchnorm_1 Batch normalization with 20 channels	Batch normalization	18×38×20	Offset 1×1×20 Scale 1×1×20
4	ReLu_1	ReLu	18×38×20	-
5	Maxpool_1 2×2 max pooling with stride [2 2] and padding [0 0 0 0]	Max pooling	9×19×20	-
6	Conv_2 20 5×5×1 convolutions with stride [1 1] and padding [0 0 0 0]	Convolution	5×15×20	Weights 5×5×20×2 Bias 1×1×20
7	Batchnorm_2 Batch normalization with 20 channels	Batch normalization	5×15×20	Offset 1×1×20 Scale 1×1×20
8	ReLu_2	ReLu	5×15×20	-
9	Maxpool_2 2×2 max pooling with stride [2 2] and padding [0 0 0 0]	Max pooling	2×7×20	-
10	Fc 3 fully connected layer	Fully connected	1×1×3	Weights 30280 Bias 3×1
11	Softmax	Softmax	1×1×3	-
12	Classoutput Crossentropyex with '1' and 2 other classes	Classification output	-	-

3.2. Model testing: first experiment

After training the CNN, to capture the iris of the eyes, we observed that the training models achieved the high scores of sensitivities = 0.97656 and specificity = 0.875. It indicates that the proposed models achieve good detection performance in the testing stage for classifying the normal and strabismus images. In this experiment, we will apply the test dataset on the trained CNN model to capture the position of the iris. This process achieved 0.95625 accuracy, which means that the CNN model can predict the classification class as Table 4. In this table, left eye and right eye indicate the predicted class number from each CNN eye model depending on iris position. We mean, each eye region (left or right eye image) is divided into three equal partitions (left, center, and right), each partition is mapped to a specific class number (1: left, 0: normal, and 2: right). In addition, target class indicates the strabismus class number (0: no strabismus, and 1: strabismus) based on the left and right eye iris class number. Moreover, the statistical measurements on the testing dataset results are Table 5.

3.3. Model testing: second experiment

The training models of CNN are used to classify deeply both eyes' images into three classes (normal, exotropia, and esotropia) as Table 6. In this figure, the decision classes represent three types of horizontal strabismus problems. As mentioned earlier, the images from three datasets are labeled by ophthalmologists. These images are classified into three classes (1, 2, and 3) to determine the direction of the person's eye looks. Class 1 indicates to the eye in front of the camera. Class 2 is related to the eye on the right side of the camera. Lastly, class 3 refers to the eye on the left side of the camera. The classification accuracy was 95:62% showing the comparison of the output and the label of the eye image. Table 6 shows the strabismus status of the person's eyes from the labeled image.

Table 4. Types of strabismus state according to left and right iris positions

Left eye	Right eye	Target class	Decision
1	1	0	No strabismus
1	2	1	Strabismus
1	3	1	Strabismus
2	1	1	Strabismus
2	2	0	No strabismus
2	3	1	Strabismus
3	1	1	Strabismus
3	2	1	Strabismus
3	3	0	No strabismus

Table 5. Performance summary of the proposed algorithm based on strabismus dataset

Architectures	TP	TN	FP	FN	Se	SP	Acc
Network	125	28	4	3	0.97656	0.875	0.95625

Table 6. Status of eyes strabismus types based on eyes classes

Left eye	Right eye	Decision
1	1	Normal
1	2	Exotropia
1	3	Esotropia
2	1	Esotropia
2	2	Normal
2	3	Binocular squint
3	1	Exotropia
3	2	Binocular divergent
3	3	Normal

3.4. Comparisons with other studies

The performance of the proposed method was experimentally compared with other studies in the related field. The comparison results are as Table 7. In this table, the column of the study represents various studies with different datasets. Some of these studies have 94% for 45 pictures of the patient. Our system exhibited an accuracy of 95:62% for three datasets of 285 images.

Table 7. Comparison with other studies

Study	Nb. of patient's images	Accuracy (%)
Almeida <i>et al.</i> [11]	45 images	94
Valente <i>et al.</i> [12]	15 videos from 15 patients	93.33
Proposed Study	285 images	95.62

4. CONCLUSIONS

Strabismus has become an influential ophthalmologic disease in human life. It plays an important role in the prognosis and treatment of strabismus. Automated detection is an effective method to achieve the suitable detection of strabismus. Concretely, automated detection is applied to attain rapid strabismus detection, which means collecting the medical data and then sending the data to specialists for physical diagnosis and examination. Three data sets on strabismus are considered in this article. In addition, all the images collected are tagged by specialists in ophthalmology. In addition, a deep learning technique using CNN model was applied for automatic detection of strabismus. The study method first uses the viola-jones algorithm to segment the eye region, and then classifies the segmented regions as strabismus using CNN. The CNN result classes are considered as inputs to two experiments. The latters were proposed in the acquisition of the position of the iris. A first experiment uses an artificial neural network to train sequenced ocular regions in order to predict the existance of strabismus or not class as a function of matching the iris position in both eyes in one hand. In the other hand, the second experiment is for predict the type of strabismus (i.e. normal, exotropia, and esotropia). The obtained results from the proposed method are promising and the results from the experiments show highly applicable rates on the automatic detection of strabismus for medical applications. For future work, we need to investigate other types of strabismus such as the V shape and the vertical strabismus, and to investigate more clinical cases.




ACKNOWLEDGEMENTS

The authors thank Mustansiriyah University, College of Science, Computer Science Department at (<http://uomustansiriyah.edu.iq>) for supporting the outcomes of this study.




REFERENCES

- [1] J. Shah and S. Patel, "Strabismus: -symptoms, pathophysiology, management & precautions," *International Journal of Science and Research*, vol. 4, no. 7, pp. 1510–1514, 2015. [Online]. Available: https://www.ijsr.net/get_abstract.php?paper_id=SUB156659
- [2] B. J. Forbes and G. E. Quinn, "Pediatric extraocular muscle surgery and oculoplastic disorders," in *Pediatric Oculoplastic Surgery*, Cham: Springer International Publishing, 2018, pp. 193–205, doi: 10.1007/978-3-319-60814-3_11.
- [3] M. J. Hockenberry and D. Wilson, *Wong's nursing care of infants and children-E-book*. 2018.
- [4] E. L. Smith, L. -F. Hung, B. Arumugam, J. M. Wensveen, Y. M. Chino, and R. S. Harwerth, "Observations on the relationship between anisometropia, amblyopia and strabismus," *Vision Research*, vol. 134, pp. 26–42, 2017, doi: 10.1016/j.visres.2017.03.004.
- [5] A. Ambastha, R. Kusumesh, S. Sinha, B. Sinha, and G. Bhasker, "Causes of visual impairment in applications for blindness certificates in a tertiary center of Bihar and its role in health planning," *Indian Journal of Ophthalmology*, vol. 67, no. 2, pp. 204–208, 2019, doi: 10.4103/ijo.IJO_837_18.
- [6] Z. Chen, H. Fu, W. -L. Lo, and Z. Chi, "Strabismus recognition using eye-tracking data and convolutional neural networks," *Journal of Healthcare Engineering*, vol. 2018, pp. 1–9, 2018, doi: 10.1155/2018/7692198.
- [7] D. Huang, A. L. Murphree, and H. Ishikawa, "System and methods for documenting and recording of the pupillary red reflex test and corneal light reflex screening of the eye in infants and young children," *U.S. Patent*, no. 9,380,938, 2016. [Online]. Available: <https://patentimages.storage.googleapis.com/b8/7a/55/8ca7e4987fc4f3/US9380938.pdf>
- [8] K. Horner, E. Wagner, and J. Tufano, "Electronic consultations between primary and specialty care clinicians: early insights," *Issue Brief (Commonw Fund)*, vol. 23, pp. 1–14, 2011. [Online]. Available: <https://core.ac.uk/download/pdf/71358065.pdf>
- [9] T. R. Attada, M. Deepika, and S. Laxmi, "Strabismus in paediatric age (3-16 year): a clinical study," *International Journal of Research in Medical Sciences*, vol. 4, no. 6, pp. 1903–1909, 2016, doi: 10.18203/2320-6012.ijrms20161731.
- [10] S. E. Loudon, C. A. Rook, D. S. Nassif, N. V. Piskun, and D. G. Hunter, "Rapid, high-accuracy detection of strabismus and amblyopia using the pediatric vision scanner," *Investigative Ophthalmology & Visual Science*, vol. 52, no. 8, pp. 5043–5048, 2011, doi: 10.1167/iovs.11-7503.
- [11] J. D. S. de Almeida, A. C. Silva, A. C. de Paiva, and J. A. M. Teixeira, "Computational methodology for automatic detection of strabismus in digital images through Hirschberg test," *Computers in Biology and Medicine*, vol. 42, no. 1, pp. 135–146, 2012, doi: 10.1016/j.compbiomed.2011.11.001.
- [12] T. L. A. Valente, J. D. S. de Almeida, A. C. Silva, J. A. M. Teixeira, and M. Gattass, "Automatic diagnosis of strabismus in digital videos through cover test," *Computer Methods and Programs in Biomedicine*, vol. 140, pp. 295–305, 2017, doi: 10.1016/j.cmpb.2017.01.002.
- [13] Z. H. Chen, H. Fu, W. L. Lo, Z. Chi, and B. Xu, "Eye-tracking-aided digital system for strabismus diagnosis," *Healthcare Technology Letters*, vol. 5, no. 1, pp. 1–6, 2018, doi: 10.1049/htl.2016.0081.
- [14] I. Piyarisi, D. Piyadigama, V. Rajapakse, A. Shanmugarajah, N. Samaranayake, and K. Shamika, "Speculo: Pattern recognition with a deep convolutional inverse graphics network for face-indexing," in *2020 IEEE International Conference for Innovation in Technology (INOCON)*, 2020, pp. 1–4, doi: 10.1109/INOCON50539.2020.9298340.
- [15] G. E. Hinton, "Learning to represent visual input," *Philosophical Transactions of the Royal Society B: Biological Sciences*, vol. 365, no. 1537, 2010, doi: 10.1098/rstb.2009.0200.
- [16] Y. Bengio, A. Courville and P. Vincent, "Representation Learning: A Review and New Perspectives," in *IEEE Transactions on Pattern Analysis and Machine Intelligence*, vol. 35, no. 8, pp. 1798–1828, 2013, doi: 10.1109/TPAMI.2013.50.
- [17] M. Kaur, T. Garg, R. Wason, and V. Jain, "Novel framework for handwritten digit recognition through neural networks," *3C Tecnología. Glosas de innovación aplicadas a la pyme*, pp. 448–467, 2019. [Online]. Available: https://www.3ciencias.com/wp-content/uploads/2019/05/eem17052019_22-1-1.pdf
- [18] Z. Fan, J. Lu, M. Gong, H. Xie and E. D. Goodman, "Automatic Tobacco Plant Detection in UAV Images via Deep Neural Networks," in *IEEE Journal of Selected Topics in Applied Earth Observations and Remote Sensing*, vol. 11, no. 3, pp. 876–887, 2018, doi: 10.1109/JSTARS.2018.2793849.
- [19] P. Liskowski and K. Krawiec, "Segmenting Retinal Blood Vessels With Deep Neural Networks," in *IEEE Transactions on Medical Imaging*, vol. 35, no. 11, pp. 2369–2380, 2016, doi: 10.1109/TMI.2016.2546227.
- [20] Y. Zhou, H. Mao, and Z. Yi, "Cell mitosis detection using deep neural networks," *Knowledge-Based Systems*, vol. 137, pp. 19–28, 2017, doi: 10.1016/j.knosys.2017.08.016.
- [21] K. Somasundaram and S. Vijayalakshmi, "A novel method for segmentation of the Hippocampus based on watershed algorithm," *2010 Second International conference on Computing, Communication and Networking Technologies*, 2010, pp. 1-6, doi: 10.1109/ICCCNT.2010.5591880.
- [22] K. Vikram and S. Padmavathi, "Facial parts detection using Viola Jones algorithm," *2017 4th International Conference on Advanced Computing and Communication Systems (ICACCS)*, 2017, pp. 1-4, doi: 10.1109/ICACCS.2017.8014636.
- [23] H. Shamil, B. Al Kindy, and A. H. Abbas, "Detection of Iris localization in facial images using haar cascade circular hough transform," *Journal of Southwest Jiaotong University*, vol. 55, no. 4, 2020, doi: 10.35741/issn.0258-2724.55.4.5.
- [24] J. D. Kelleher, *Deep learning*. The MIT Press, 2019, doi: 10.7551/mitpress/11171.001.0001.
- [25] Y. -L. Boureau, J. Ponce, and Y. LeCun, "A theoretical analysis of feature pooling in visual recognition," in *in Proceedings of the 27th international conference on machine learning (ICML-10)*, 2010. [Online]. Available: <https://www.di.ens.fr/willow/pdfs/icml2010b.pdf>
- [26] V. Nair and G. E. Hinton, "Rectified linear units improve restricted boltzmann machines," in *Icml*, 2010. [Online]. Available: <https://icml.cc/Conferences/2010/papers/432.pdf>
- [27] A. Krizhevsky, I. Sutskever, and G. E. Hinton, "Imagenet classification with deep convolutional neural networks," *Communications of the ACM*, vol. 60, no. 6, pp. 84–90, 2017, doi: 10.1145/3065386.
- [28] T. Sledovic, "Adaptation of Convolution and Batch Normalization Layer for CNN Implementation on FPGA," *2019 Open Conference of Electrical, Electronic and Information Sciences (eStream)*, 2019, pp. 1-4, doi: 10.1109/eStream.2019.8732160.
- [29] L. Bottou, "Stochastic Gradient Descent Tricks," *Neural Networks: Tricks of the Trade*, Berlin, Heidelberg: Springer, 2012, doi: 10.1007/978-3-642-35289-8_25.
- [30] T. Fawcett, "An introduction to ROC analysis," *Pattern Recognition Letters*, vol. 27, no. 8, pp. 861–874, 2006, doi: 10.1016/j.patrec.2005.10.010.




BIOGRAPHIES OF AUTHORS

Haider Shamil Hamid    is a graduate M.Sc. student in Computer Science. He received his Bachelor in Computer science from Mustansiriyah University (Iraq), 2016. He can be contacted at email: haidershamil@gmail.com.






Bassam AlKindy    is a doctor in Computer Science. He received his M.Sc. degree in Computer Science from Yarmouk University, faculty of information Technology and Computer Science (Jordan), 2005. In 2015, he obtained a Ph.D. degree in Computer Science - Artificial Intelligence - bioinformatics from the University of Franche-Comt' e, Lab. Femto-ST (DISC, Department of computer science), France. His researches focus on the domains of Artificial Intelligent, Bioinformatics (Ancestor reconstruction and phylogenetic analysis), Robotics, and Machine learning. He can be contacted at email: dr.balkindy@uomustansiriyah.edu.iq.



Amel H. Abbas    is an assistant professor doctor in Mustansiriyah University. She received her B.Sc. and M.Sc. degrees in Physics from Mustansiriyah University (Iraq), 1988 and 1996 respectively. She received her Ph.D. degree in 2003 from the University of Baghdad in the field of Image Processing. Her research interests include image processing and image classification with Matlab programming. She is an assistant professor in Mustansiriyah University. Skills Image Processing Pattern Recognition Computer Vision MATLAB. She can be contacted at email: dr.amelhussein2017@uomustansiriyah.edu.iq.



Wissam Basim Al-Kendi    holds M.Sc. degree in computer science from the University of Nottingham in the UK, and a Bachelor's degree in computer science and information system from the University of Technology, Iraq. Currently, he works as a senior programmer and department director assistant at the Federal Commission of Integrity in Iraq. His research work focus on the domain of artificial intelligent, optimization, and machine learning. He can be contacted at email: wisksam@gmail.com.